

Quantum shift of band-edge stimulated emission in InGaN–GaN multiple quantum well light-emitting diodes

C. J. Sun, M. Zubair Anwar, Q. Chen, J. W. Yang, M. Asif Khan, M. S. Shur, A. D. Bykhovski, Z. Liliental-Weber, C. Kisielowski, M. Smith, J. Y. Lin, and H. X. Jiang

Citation: *Applied Physics Letters* **70**, 2978 (1997); doi: 10.1063/1.118762

View online: <http://dx.doi.org/10.1063/1.118762>

View Table of Contents: <http://scitation.aip.org/content/aip/journal/apl/70/22?ver=pdfcov>

Published by the [AIP Publishing](#)

Instruments for advanced science

Gas Analysis



- dynamic measurement of reaction gas streams
- catalysis and thermal analysis
- molecular beam studies
- dissolved species probes
- fermentation, environmental and ecological studies

Surface Science



- UHV TPD
- SIMS
- end point detection in ion beam etch
- elemental imaging - surface mapping

Plasma Diagnostics



- plasma source characterization
- etch and deposition process
- reaction kinetic studies
- analysis of neutral and radical species

Vacuum Analysis



- partial pressure measurement and control of process gases
- reactive sputter process control
- vacuum diagnostics
- vacuum coating process monitoring

contact Hiden Analytical for further details

HIDEN
ANALYTICAL

info@hideninc.com
www.HidenAnalytical.com

CLICK to view our product catalogue



Quantum shift of band-edge stimulated emission in InGaN–GaN multiple quantum well light-emitting diodes

C. J. Sun, M. Zubair Anwar, Q. Chen, J. W. Yang, and M. Asif Khan
APA Optics Inc., 2950 N. E. 84th Lane, Blaine, Minnesota 55434

M. S. Shur
Department of Electrical, Computer, and Systems Engineering, Rensselaer Polytechnic Institute, Troy, New York 12180-3590

A. D. Bykhovski^{a)}
Department of Electrical Engineering, University of Virginia, Charlottesville, Virginia 22903-2442

Z. Liliental-Weber
Lawrence Berkeley National Laboratory, Berkeley, California 94720

C. Kisielowski
Department of Materials Science and Mineral Engineering, University of California at Berkeley, Berkeley, California 94720

M. Smith, J. Y. Lin, and H. X. Jiang
Department of Physics, Kansas State University, Manhattan, Kansas 66506

(Received 30 May 1996; accepted for publication 29 March 1997; corrected 03 March 2011)

We report on the band-edge stimulated emission in InGaN–GaN multiple quantum well light-emitting diodes with varying widths and barrier thicknesses of the quantum wells. In these devices, we observe that the stimulated emission peak wavelength shifts to shorter values with decreasing well thickness. From the comparison of the results of the quantum mechanical calculations of the subbands energies with the measured data, we estimate the effective conduction- and valence-band discontinuities at the GaN–In_{0.13}Ga_{0.87}N heterointerface to be approximately 130–155 and 245–220 meV, respectively. We also discuss the effect of stress on the estimated values of band discontinuities. © 1997 American Institute of Physics. [S0003-6951(97)00722-5]

Recently, much interest has focused around the use of high quality epilayers and heterojunctions of the AlGaIn–InGaIn material systems for lasing structures.¹ In the past, several groups^{2,3} including ours⁴ have demonstrated optically pumped stimulated emission using high quality single layers or single heterojunctions of GaN–InGaIn. In this letter, we report on the band-edge stimulated emission in InGaIn–GaIn multiple quantum well (MQW) light-emitting diodes with varying widths and barrier thicknesses of the quantum wells (QWs). In these devices, we observe that the stimulated emission peak wavelength shifts to shorter values with decreasing well thickness. From this measured quantum shift, we estimate the effective conduction- and valence-band discontinuities at the heterointerface. These values are important for the design of GaN based electronic and optoelectronic heterostructure devices.

In this work, we used low-pressure switched atomic layer epitaxy for the deposition of the MQW structures. The MQWs were deposited over basal plane sapphire substrates using low-pressure metalorganic chemical vapor deposition. Triethylgallium, trimethylindium, and ammonia were used as precursors for all InGaIn and GaIn growths. The GaIn and InGaIn depositions were carried out at 750 °C and 500 Torr. Typical precursor flows were similar to those described earlier.⁵

The structure consisted of an approximately 1 μm thick GaIn layer followed by the MQW region. The individual layer thicknesses for the MQW regions for the samples of the

stimulated emission study are listed in Table I. Indium composition in the well region was kept at $x=0.13$. The total thickness of InGaIn in the MQW region (number of periods times the well thickness) was also kept constant, thereby, insuring a fixed pumped volume of InGaIn for the different MQWs. From our past work, we estimate the penetration depth of the nitrogen laser (337 nm) to be around 0.2 μm for GaIn (and/or) In_{0.13}Ga_{0.87}N, which is considerably larger than the total MQW thicknesses for the samples of this study. We used x-ray analysis to study the structure quality and verify quantum well thickness. From the position of the higher-order x-ray diffraction peaks, we estimated the thicknesses of one period (barrier and well) to be approximately 80 Å for sample II of Table I. This is in reasonable agreement with the values based on growth parameters. To further confirm the quantum well thicknesses and to have a closer look at the interface quality, we used cross-sectional high-resolution transmission electron microscopy (TEM).

The designed thickness of the TEM sample, which was

TABLE I. Summary of growth parameters of different MQWs for quantum shift experiments of band-edge stimulated emission.

Sample No.	Well width (Å)	Barrier width (Å)	Number of periods	Total In _x Ga _{1-x} N thickness (Å)
I	Single layer	...	1	250
II	25	50	10	250
III	12.5	25	20	250
IV	5	10	50	250
TEM study	50	50	10	500

^{a)}On leave from A. F. Ioffe Institute of Physics and Technology, 194021 St., Petersburg, Russia.

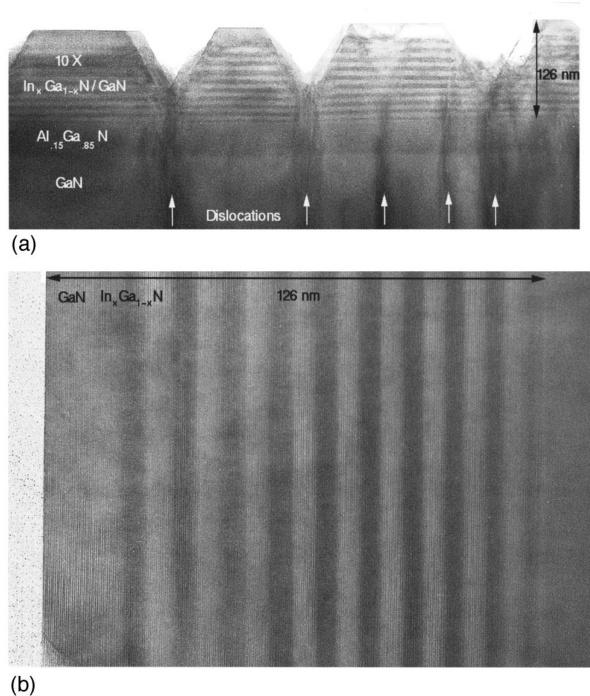


FIG. 1. Cross-sectional TEM micrographs of InGaN/GaN MQWs. (a) shows the TEM image that reveals truncated triangle-like surface morphology at lower magnification, and (b) is the lattice image that shows the gradual increase of quantum well thickness at higher magnification.

grown under similar conditions as sample II, is also listed in Table I. An indium concentration ($x=0.35$), larger than in the other samples was grown into the structure. The TEM images [Figs. 1(a) and 1(b)] depict that GaN/ $\text{In}_x\text{Ga}_{1-x}\text{N}$ /GaN quantum well structures can be grown with a reasonable homogeneous In concentration in the wells and with well-defined interfaces that are abrupt. The GaN/ $\text{In}_x\text{Ga}_{1-x}\text{N}$ and the $\text{In}_x\text{Ga}_{1-x}\text{N}$ /GaN extend over a distance of 1–1.5 nm across the QW's.⁶ No misfit dislocations are formed during growth of the wells. The spacing of the GaN/ $\text{In}_x\text{Ga}_{1-x}\text{N}$ stacks is regular. It ranges from 10 to 11 nm for quantum wells close to the substrate (stack 1–6, counted from the substrate side) and increases only slightly to 13 nm in the top of the structure (stack 7–10). The data are in reasonable agreement with x-ray measurements and with estimations based on growth parameters. Clearly, strain relaxation occurred via surface roughening, which led to the three-dimensional growth in the top of the structure forming facets with a V-shape on the $\{01\ 11\}$ planes [Fig. 1(a)]. Formation of the facets on these polar planes might have the same origin as formation of pinholes observed in GaN.⁷ This occurred at an effective $\text{In}_x\text{Ga}_{1-x}\text{N}$ layer thickness of 25 nm for an indium concentration of $x=35\%$. Details about relaxation processes will be published elsewhere.⁶ Here, we note that in the structures used for our optical measurements, the low In concentration of $x=13\%$ assures that this critical thickness for strain relaxation is not exceeded. It is for this reason that the indium concentration in our $\text{In}_x\text{Ga}_{1-x}\text{N}$ layers with $x=13\%$ is more homogeneous and that no surface roughening occurred. On the other hand, the shape of the In concentration profile across our short period superlattice with a well width of 1.25 or even 0.5 nm will certainly be domi-

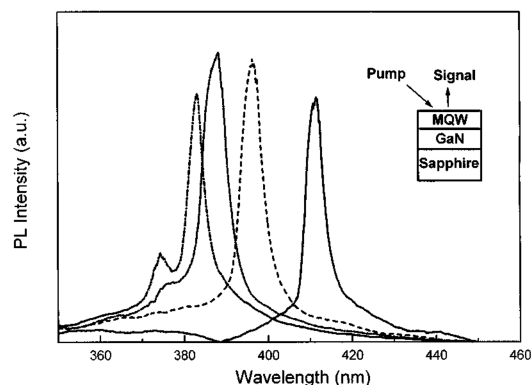


FIG. 2. Measured stimulated emission from GaN/ $\text{In}_{0.13}\text{Ga}_{0.87}\text{N}$ multiple quantum wells at room temperature. $(25\ \text{\AA}/50\ \text{\AA}) \times 10$ periods MQW (dashed line), $(12.5\ \text{\AA}/25\ \text{\AA}) \times 20$ periods (dotted line) MQW, and $(5\ \text{\AA}/10\ \text{\AA}) \times 50$ periods MQW (dashed-dotted line). Emission from the bulk $\text{In}_{0.13}\text{Ga}_{0.87}\text{N}$ (solid line). The inset shows the vertical cavity configuration for the optical pumping experiments.

nated by the final $\text{In}_x\text{Ga}_{1-x}\text{N}$ /GaN interfacial width of 1–1.5 nm.

In Fig. 2, we plot the room-temperature pulsed photoluminescence (PL) of the samples of Table I along with that of a bulk $250\ \text{\AA}$ thick $\text{In}_{0.13}\text{Ga}_{0.87}\text{N}$ sample. A nitrogen laser operating at 337 nm and a vertical cavity geometry were used for these measurements (see the inset in Fig. 2). The laser beam was focused on the sample to yield a maximum power density of $10\ \text{MW}/\text{cm}^2$. A synchronous boxcar detection system with a photomultiplier tube was used to measure PL signals. As before,^{4,5} we assign the sharp emission peaks (full width at half-maximum = 3 nm) to the onset of the stimulated emission (the threshold power was $1\ \text{MW}/\text{cm}^2$).

The stimulated emission peak clearly moves to shorter wavelengths with decreasing well thicknesses. We feel the shift in the stimulated emission peak position to be caused by quantum confinement, and is related to the subband formation in the quantum wells. This allows us to estimate the conduction-band and the valence-band discontinuities, ΔE_c and ΔE_v . Since the electron effective mass in $\text{In}_{0.13}\text{Ga}_{0.87}\text{N}$ is much smaller than the heavy-hole mass, the quantum shift is larger when a larger fraction of the energy-band discontinuity $\Delta E_g = \Delta E_c + \Delta E_v$ is in the conduction band. By comparing the calculated shift with the measured value, we can extract an approximate value of band discontinuities. To this end, we first estimated the electron effective mass of $\text{In}_{0.13}\text{Ga}_{0.87}\text{N}$ as follows:

$$m^*/m_0 = 0.11 + 0.09(1 - x). \quad (1)$$

From our photoluminescence data, we estimated the band gap of the bulk $\text{In}_{0.13}\text{Ga}_{0.87}\text{N}$ to be 3.024 eV, in approximate agreement with the data of Osamura *et al.*⁸ We then calculated the positions of the first subbands for electrons and heavy holes for the composition profiles corresponding to our MQW listed in Table I. For these calculations, we used a software program called 1DPoisson, which solves self-consistently the Schrodinger and Poisson equations. We also checked that the results of these calculations are in good agreement with approximate calculations based on the Kronig–Penney model. For $\Delta E_c/\Delta E_v = 0.5\text{--}0.7$, we obtained the positions of the peaks approximately 398 and 390

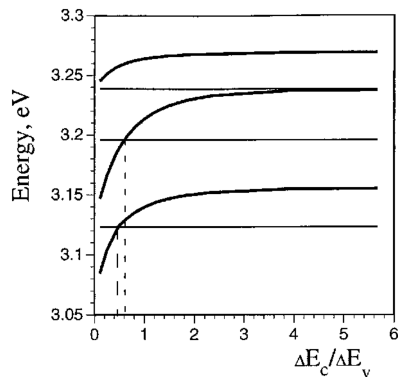


FIG. 3. Calculated lowest-electron-band-highest-heavy-hole-band transition in the GaN/In_{0.13}Ga_{0.87}N MQW as a function of conduction-band-valence-band offset ratio. From bottom to top, 25 Å/50 Å well/barrier, 12.5 Å/25 Å well/barrier, 5 Å/10 Å well/barrier. Horizontal lines mark the positions of the corresponding experimental emission peaks from Fig. 2.

nm for the structures with 25 Å quantum wells and 12.5 Å quantum wells, respectively, in agreement with the measured peaks (see Fig. 2). Even though the quality of our structure with the 5 Å quantum wells was the same as the quality of our structures with wider wells, the fit with the simple theory based on the effective-mass approximation could not be obtained (see Fig. 3). This is not surprising, because the effective-mass approximation is not valid for such short period superlattices.⁹ As it was shown in Ref. 9 for wurtzite III-nitride superlattices, the calculations based on the effective-mass approximation overestimate the changes in the energy levels in III-nitrides due to confinement.

The wide-band-gap semiconductors exhibit pronounced piezoelectric properties.^{10,11} The piezoeffect can cause the electron-hole spatial separation and dramatically change the selection rules for the interband transitions by reducing the optical matrix element for the lowest-conduction-band-first-heavy-hole transition and by allowing transitions forbidden for flatbands. Also, it can cause an apparent decrease of the band gap. In our estimates, we neglected the piezoeffect for the following reasons: The nonequilibrium carrier concentrations generated by optical pumping are on the order of 10¹⁹ cm⁻³ or more. At these concentrations, the strain-induced electric field is largely reduced for our structures. Therefore, for the short-period superlattices, with the quantum wells of 25 or shorter, the effect of the built-in electric field on the band structure will be negligible. (For wider layers, this may not be true even at high carrier concentrations.)

Figure 4 shows the computed band diagram of the GaN/In_{0.13}Ga_{0.87}N superlattice with 25 Å quantum wells and 50 Å barriers. We estimated the discontinuities to be 130–155 meV and 245–220 meV for the conduction and the valence band, respectively.

Our estimate of the conduction-valence-band offset ratio, 0.5–0.7, is close to that extracted from the photoemission for InN/GaN heterostructures (for InN/GaN, the ratio is roughly 0.8).¹² However, additional studies of optical spectra and current-voltage and capacitance-voltage characteristics of GaN-InGaN structures are needed for a more accurate estimate of the band-edge discontinuities.

In conclusion, we report on a room-temperature stimulated emission of GaN-In_{0.13}Ga_{0.87}N multiple quantum wells

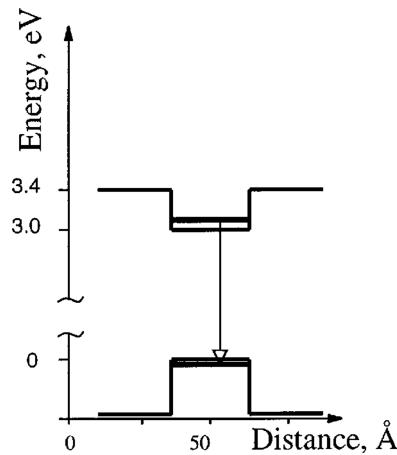


FIG. 4. Computed band diagram of the GaN/In_{0.13}Ga_{0.87}N MQW. 25 Å quantum wells and 50 Å barriers. Horizontal solid lines are subband energies. Only one period of the structure and the lowest transition are shown.

grown over basal plane sapphire substrates. In these devices, we observed the quantum shift related to the subband energy dependence on the well thickness and estimated the effective conduction-band discontinuity at the GaN-In_{0.13}Ga_{0.87}N heterointerface to be approximately 130–155 meV, and 245–220 meV for the valence-band discontinuity, correspondingly. The estimated ratio of the conduction-band discontinuity-to-valence-band discontinuity, 0.5–0.7, is close to that extracted from the photoemission for InN/GaN heterostructures.¹²

This work was partially supported by Air Force Contract No. F33615-94-C-1444 and was monitored by Mr. Don Agresta of WPAFB. It was also partially supported by DARPA Contract No. N00014-95-C-0073 and was monitored by Dr. Y. S. Park of the Office of Naval Research. Work at the Rensselaer Polytechnic Institute and at the University of Virginia has been supported by the Office of Naval Research under Contract No. N00014-92-C-0090 and was monitored by Dr. Colin Wood. TEM work was supported by the BMDO GaN Microwave Power Amplifier Project administered by ONR under Contract No. N00014-96-1-0901. Two of the authors, Z.L.W. and C.K., want to acknowledge the National Center for Electron Microscopy at LBNL in Berkeley for the use of their facility.

¹S. Nakamura, M. Senoh, N. Iwasa, S. Nagahama, T. Yamada, T. Matushita, H. Kiyoko, and Y. Sugimoto, *Jpn. J. Appl. Phys.* **2**, Lett. **35**, L74 (1996).

²S. T. Kim, H. Amano, and I. Akasaki, *Appl. Phys. Lett.* **67**, 267 (1995).

³X. H. Yang, T. J. Schmidt, W. Shan, and J. J. Song, *Appl. Phys. Lett.* **66**, 1 (1995).

⁴M. A. Khan, S. Krishankutty, R. A. Skogman, J. N. Kuznia, D. T. Olson, and T. George, *Appl. Phys. Lett.* **65**, 520 (1994).

⁵C. J. Sun, J. W. Yang, Q. Chen, B. W. Lim, M. Z. Anwar, M. A. Khan, H. Temkin, D. Weismann, and I. Brenner, *Appl. Phys. Lett.* **69**, 668 (1996).

⁶C. Kisielowski, Z. Liliental-Weber, J. Yang, and A. Khan (unpublished).

⁷Z. Liliental-Weber, Y. Chen, S. Ruvimov, and J. Washburn, *Phys. Rev. Lett.* (submitted).

⁸K. Osamura, K. Nakajima, Y. Murakami, P. H. Shingu, and A. Atsuki, *Solid State Commun.* **11**, 617 (1972).

⁹S. Y. Ren and J. D. Dow, *Mater. Res. Soc. Symp. Proc.* **281**, 775 (1993).

¹⁰A. Bykhovski, B. Gelmont, and M. Shur, *J. Appl. Phys.* **74**, 6734 (1993).

¹¹A. D. Bykhovski, V. V. Kaminski, M. S. Shur, Q. C. Chen, and M. A. Khan, *Appl. Phys. Lett.* **68**, 818 (1996).

¹²G. Martin, A. Botchkarev, A. Rockett, and H. Morko, *Appl. Phys. Lett.* **86**, 2541 (1996).